Research Article

# Scalable Antigen-Antibody Binding Affinity Landscape: A Case Study with ENHERTU

**Wei Li**[1]

1. Contrebola Institute of Computational Inter-structural Biophysics, China

**Optimization of binding affinities for antibody-drug conjugates (ADCs) is crucial for their therapeutic efficacy and specificity, with most ADCs engineered to achieve equilibrium dissociation constants in the range of 0.1 to 1 nM. However, there is a lack of published data delineating the optimal binding affinity range that ensures improved therapeutic outcomes for ADCs. Therefore, this study integrates structural biophysics within a scalable in silico workflow to generate antigen-antibody binding affinity landscapes, focusing on ENHERTU, a monoclonal antibody employed in the treatment of HER2-positive breast cancer. Leveraging computational techniques, including homology structural modeling and structural biophysics-based binding affinity calculations, this article presents high-accuracy structural and intermolecular binding affinity data for the Her2-Trastuzumab-Pertuzumab complex. Beyond the design of Her2-targeting ADCs with enhanced efficacy and specificity, this scalable antigen-antibody binding affinity landscape offers a technically feasible workflow for the high-throughput generation of synthetic structural and biophysical data with reasonable accuracy. Combined with artificial intelligence (AI) algorithms, it is conceivable that this scalable in silico approach constitutes a catalyst for an AI-driven paradigm shift in the discovery and design of antibodies and ADCs with improved efficacy and specificity.**

**Significance: This study presents a structural biophysics-based search engine tailored for ranking antigen-antibody binding affinities, with a specific focus on ENHERTU, a key monoclonal antibody in HER2-positive breast cancer treatment. By integrating advanced computational techniques like homology structural modeling and $K_d$ calculations, the research generates accurate structural and binding affinity data. This scalable approach not only enhances the design of next-generation antibody-drug conjugates (ADCs) but also provides a practical method for generating synthetic structural and biophysical data efficiently. Combined with artificial intelligence algorithms, this**

 doi.org/10.32388/I2P70W 

**scalable in silico approach aims to catalyze a paradigm shift in the discovery and design of antibodies and ADCs with improved efficacy and specificity.**

**Corresponding author:** Wei Li, wli148@aucklanduni.ac.nz

## Introduction

Antibody-drug conjugates (ADCs) represent a rapidly advancing class of targeted cancer therapies that merge the specificity of monoclonal antibodies with the potent cytotoxicity of small molecule drugs[1][2]. These biopharmaceuticals are designed to selectively deliver therapeutic agents (i.e., payloads) to cancer cells, thereby minimizing off-target effects and enhancing treatment efficacy[3][4]. To date, drug discovery and design remain a complex multiparameter optimization challenge[5][6]. For instance, central to the efficacy and specificity of ADCs is the binding interaction between the antibody and its target antigen, where the physical strength of this binding is typically quantified as the antigen-antibody equilibrium dissociation constant ($K_d$)[7][8]. The $K_d$ of ADCs to their target antigens is a critical determinant of receptor-mediated endocytosis and, consequently, the therapeutic efficacy of ADCs[9]. ADCs with high binding affinity are more efficiently internalized, as strong binding ensures that the ADC remains attached to the antigen long enough for the endocytic machinery to recognize and internalize the ADC-antigen complex. This leads to more effective delivery of the cytotoxic payload into tumor cells and enhanced specificity, reducing off-target effects and improving the therapeutic index. Conversely, ADCs with low binding affinity may dissociate from the antigen before endocytosis occurs, resulting in reduced internalization and decreased efficacy. Lower affinity might also increase the risk of binding to non-target molecules, leading to off-target effects. Nonetheless, extremely high antigen-antibody affinity can hinder ADC tissue penetration[10], while too low affinity can result in insufficient internalization[11]. While most ADCs aim for a $K_d$ within the nanomolar range ($10^{-9}$ to $10^{-10}$ M), few published data have solved the relationship between optimal antigen-antibody $K_d$ and the efficacy and specificity of ADCs[12][13].

As a result, this study addresses this paucity of data by developing a scalable in silico approach for structural biophysics-based calculations of antigen-antibody binding affinities, with trastuzumab as an example, a monoclonal antibody widely used in the treatment of HER2-positive breast cancer[14][15]. Experimentally determining this for ADCs poses significant challenges, as tools such as surface plasmon

resonance and isothermal titration calorimetry necessitate meticulous control of experimental conditions and the use of purified components, making these approaches rather resource- and labor-intensive[16][17][18][19]. On the other hand, computational tools offer a useful alternative approach to explore the antigen-antibody sequence space and chart out the entire territories of antigen-antibody binding affinity landscapes[20]. Thus, this study employs computational tools such as structural modeling[21] and physics-based $K_d$ calculations[22][23] to define and build a scalable antigen-antibody binding affinity ($K_d$) landscape for the design of antibodies and ADCs with improved efficacy and specificity.

## Materials and Methods

Trastuzumab deruxtecan (ENHERTU) is a HER2-directed antibody and DNA topoisomerase I inhibitor conjugate developed for the treatment of HER2-expressing solid tumours[24][25][26]. As the monoclonal antibody in ENHERTU, trastuzumab binds directly to the extracellular domain of the HER2 receptor, inhibiting its downstream signaling pathways and mediating antibody-dependent cellular cytotoxicity[14][15]. As of 2025-05-02, there is a total of 22 trastuzumab-related structures in the Protein Data Bank (PDB)[27][28], as listed in Table 1.

| PDB ID | Structure Title (release date from newest to oldest) |
|---|---|
| 8PWH | Atomic structure and conformational variability of the HER2-Trastuzumab-Pertuzumab complex |
| 8Q6J | Atomic structure and conformational variability of the HER2-Trastuzumab-Pertuzumab complex |
| 7PKL | Mechanistic understanding of antibody masking with anti-idiotypic antibody fragments |
| 7MN8 | Structure of the HER2/HER3/NRG1b Heterodimer Extracellular Domain bound to Trastuzumab Fab |
| 6OGE | Cryo-EM structure of Her2 extracellular domain-Trastuzumab Fab-Pertuzumab Fab complex |
| 6BGT | Structure of Trastuzumab Fab mutant in complex with Her2 extracellular domain |
| 6BAH | Trastuzumab Fab v3 with 5-diphenyl meditope variant |
| 6BAE | Trastuzumab Fab v3 in complex with CQFDLSTRRLKC |
| 6B9Z | Trastuzumab Fab v3 |
| 6B9Y | Trastuzumab Fab v3 in complex with 5-phenyl meditope variant |
| 5U6A | Crystal structure of I83E meditope-enabled trastuzumab with azido-peg3-meditope |
| 5U5M | Crystal structure of I83E meditope-enabled trastuzumab with azido-meditope |
| 5U5F | Meditope enabled trastuzumab I83E variant in complex with Ac) CQFDA(PH)2STRRLRCGGSK |
| 5U3D | Structure of meditope enabled trastuzumab I83E variant |
| 6BI2 | Trastuzumab Fab D185A (Light Chain) Mutant Biotin Conjugation |
| 6BI0 | Trastuzumab Fab N158A, D185A, K190A (Light Chain) Triple Mutant |
| 6BHZ | Trastuzumab Fab D185A (Light Chain) Mutant |
| 5XHG | Crystal structure of Trastuzumab Fab fragment bearing Ne-(o-azidobenzyloxycarbonyl)-L-lysine |
| 5XHF | Crystal structure of Trastuzumab Fab fragment bearing p-azido-L-phenylalanine |
| 4IOI | Meditope-enabled trastuzumab in complex with CQFDLSTRRLKC |
| 4HKZ | Trastuzumab Fab complexed with Protein L and Protein A fragments |
| 4HJG | Meditope-enabled trastuzumab |

**Table 1.** Experimentally determined trastuzumab-related structures (released newest to oldest) in PDB as of 2025-05-02, QUERY code: QUERY: Full Text = "Trastuzumab".


doi.org/10.32388/I2P70W

Among the 22, there are a total of three HER2-Trastuzumab-Pertuzumab complex structures with PDB IDs 6OGE[14]), 8PWH[15] and 8Q6J[15]. In light of the standardized PDB data format for biomolecular structures, it does not really matter which one of the three is chosen here for subsequent structural modeling[21] and physics-based $K_d$ calculations[22][23], as all three HER2-Trastuzumab-Pertuzumab complex structures are determined experimentally with Cryo-EM[14][15]. Moreover, while only trastuzumab is used in ENHERTU, a synergistic anticancer effect of the two antibodies is also likely, according to a detailed CryoEM study of the ternary complex[15]. Thus, this study here chooses PDB entry 6OGE[14]) as an example to define and build a scalable antigen-antibody binding affinity ($K_d$) landscape. Briefly, the relationships between chain IDs and molecular entities of PDB entry 6OGE are listed in Table 2, which is to be used in describing the results of the subsequent structural modeling[21] and physics-based $K_d$ calculations[22][23].

| Chain ID | Molecular entity | Length |
|---|---|---|
| A | Receptor tyrosine-protein kinase erbB-2 (Homo sapiens, 9606) | 622 |
| B | Pertuzumab FAB LIGHT CHAIN (Homo sapiens, 9606) | 214 |
| C | Pertuzumab FAB HEAVY CHAIN (Homo sapiens, 9606) | 222 |
| D | Trastuzumab FAB LIGHT CHAIN (Homo sapiens, 9606) | 214 |
| E | Trastuzumab FAB HEAVY CHAIN (Homo sapiens, 9606) | 220 |
| BC | Pertuzumab FAB (Homo sapiens, 9606) | 436 |
| DE | Trastuzumab FAB (Homo sapiens, 9606) | 434 |
| Total | PDB entry 6OGE[14] | 1492 |

**Table 2.** Relationships between chain IDs and molecular entities of PDB entry 6OGE. In this table, length represents the number of amino acid residues, and total means the entire PDB entry 6OGE[14]), i.e., A+B+C+D+E.

With PDB entry 6OGE[14] (Table 1) as an initial input, subsequent structural modeling[21] and physics-based $K_d$ calculations[22][23] consist of an automated in silico generation of synthetic homology structural and $K_d$ data, as illustrated in Figure 1 and described previously in detail[29]. Briefly, Modeller[21] was employed to build a total of 29,840 $(1,492 \times 20)$ homology structural models with one site-specific missense mutation introduced to PDB entry 6OGE[14]. Afterwards, the binding affinities were calculated using Prodigy[22][23] for all 29,840 structural models of Her2-Trastuzumab-Pertuzumab analogues, including the $K_d$ values between chains A and B, chains A and C, chains A and D, chains A and E, chains A and BC, and chains A and DE (Table 2). With PDB entry 6OGE[14] as a template, all structural modeling[21] and physics-based $K_d$ calculations[22][23] were repeated three times on Wuxi Taihu Lake High Performance Computing platforms.

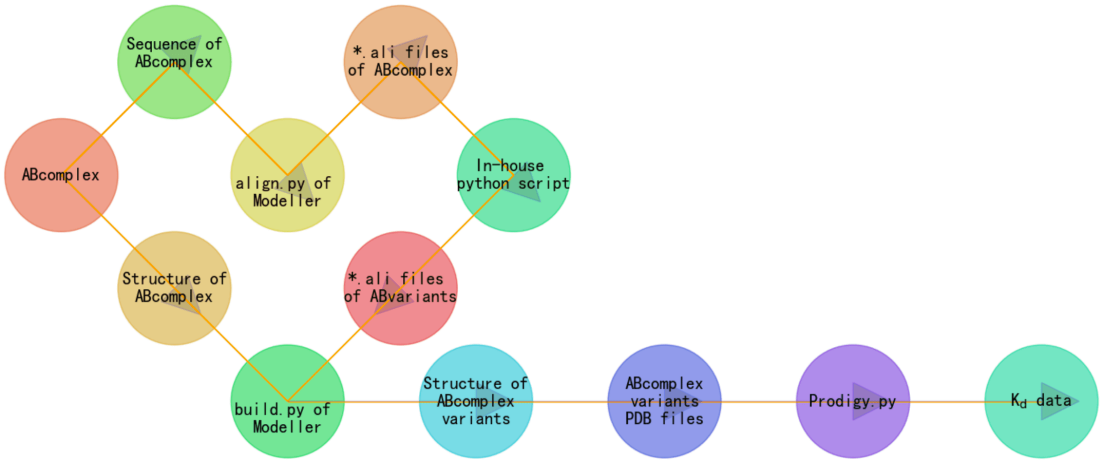


**Figure 1.** Automated in silico generation ([29]) of synthetic structural (Modeller [21]) and $K_d$ (Prodigy [22][23]) data.

Of further note, among the twenty natural amino acids, cysteine is a special one from a structural point of view, in the sense that removal of cysteine residue(s) or introduction of new cysteine residue(s) might induce a perturbation of the disulfide bonding network towards a major structural rearrangement of a protein. Yet, engineering cysteines at specific sites in antibodies has proven to be a promising approach to create well-defined ADCs for the treatment of cancer[30][31]. This study, therefore, reports a computational systematic amino acid (including cysteine) scanning[13][32][33][34][35] of the entire PDB

entry 6OGE (1492 amino acid residues, Table 2)[14] to incorporate structural biophysics (e.g., $K_d$)[8] into the property-based design of cysteine-linked ADCs[5][6].

## Results

Since this study used PDB entry 6OGE[14] as the structural template, Prodigy[22][23] was used to calculate the inter-chain binding affinities for the native experimental Her2-Trastuzumab-Pertuzumab complex structure. These physics-based calculations were performed between chains A and B, chains A and C, chains A and D, chains A and E, chains A and BC, and chains A and DE, as listed in Table 3 below.

| Binding partners | Inter-chain binding affinity (M) at 37 °C of PDB entry 6OGE |
|---|---|
| A + B | $1.4 \times 10^{-5}$ |
| A + C | $9.5 \times 10^{-8}$ |
| A + D | $8.6 \times 10^{-6}$ |
| A + E | $3.8 \times 10^{-6}$ |
| A + BC | $1.9 \times 10^{-8}$ |
| A + DE | $4.9 \times 10^{-7}$ |

**Table 3.** Inter-chain binding affinities calculated by Prodigy for the native experimental Her2-Trastuzumab-Pertuzumab complex structure PDB entry 6OGE. In this table, the codes (A, B, C, etc.) for binding partners are defined in Table 2.

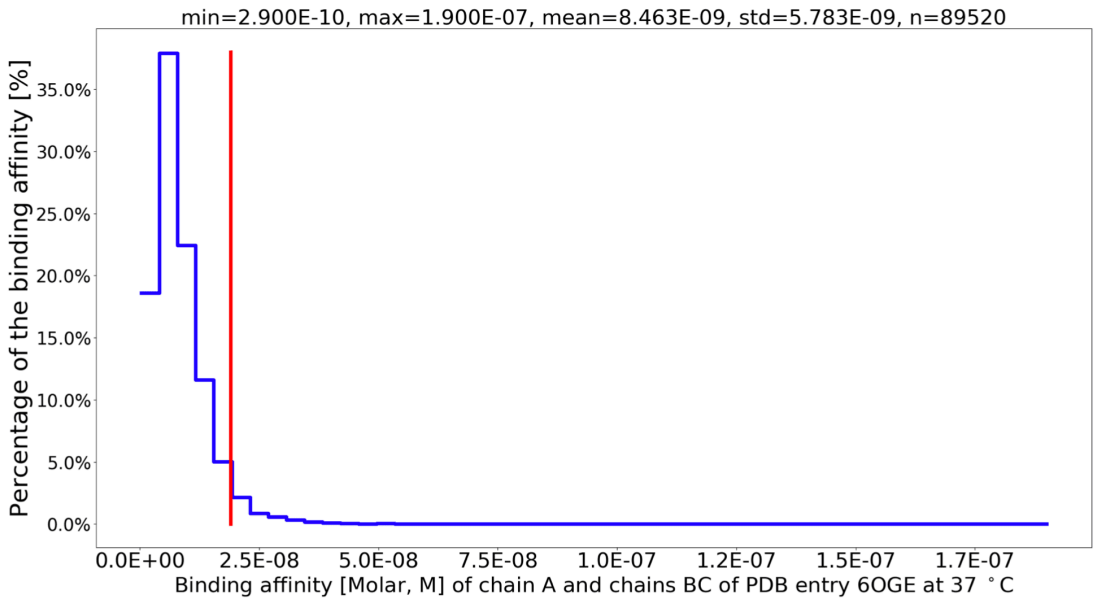


**Figure 2.** Histogram depicting the distribution pattern of the Her2-Pertuzumab binding affinities between chain A and chain BC (Table 2) of PDB entry 6OGE with one site-specific missense mutation. The vertical red line indicates the $K_d$ between chain A (Her2) and chain BC (Pertuzumab FAB), representing the native complex structure of Her2-Trastuzumab-Pertuzumab (PDB entry 6OGE).

Afterwards, with PDB entry 6OGE[14] as the structural template, this study conducted three sets of structural modeling[21] and physics-based $K_d$ calculations[22][23]. These calculations were also performed to determine $K_d$ values for interactions between chains A and B, chains A and C, chains A and D, chains A and E, chains A and BC, and chains A and DE, as detailed in Table 2. The resulting $K_d$ values and their corresponding analyses are comprehensively summarized in Table 4, with additional data presented in six supplementary tables and six figures contained in the supplementary file supps.pdf.

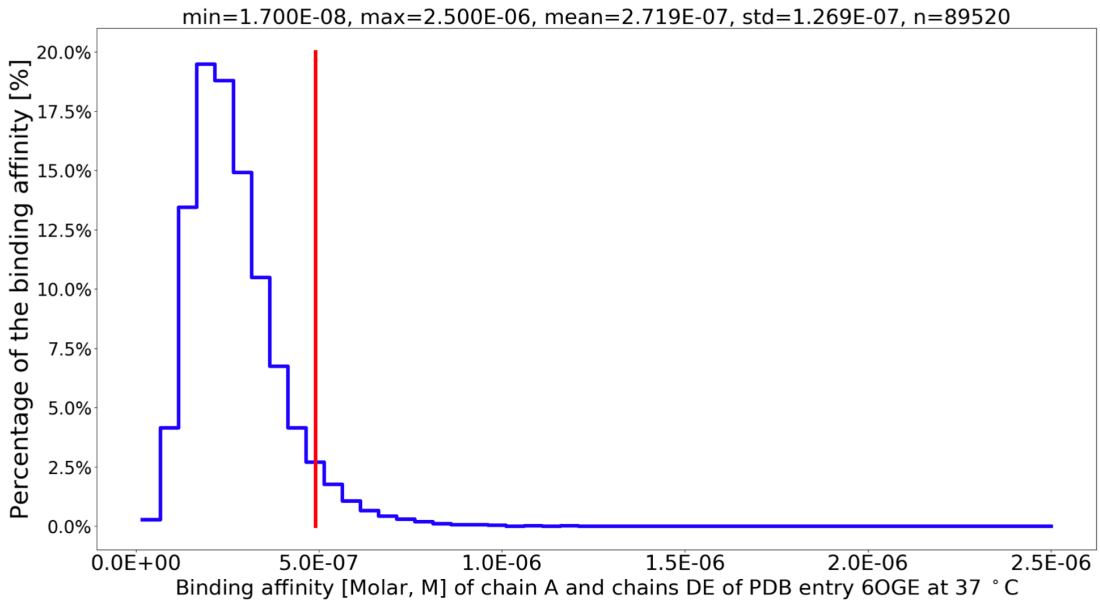


**Figure 3.** Histogram showing the distribution pattern of the Her2-Trastuzumab binding affinities between chain A and chain DE (listed in Table 2) of PDB entry 6OGE with one site-specific missense mutation. The vertical red line marks the Kd between chain A (Her2) and chain DE (Trastuzumab FAB), representing the native complex structure of Her2-Trastuzumab-Pertuzumab (PDB entry 6OGE).

According to Table 3, the $K_d$ between Her2 and pertuzumab Fab is located at $1.9 \times 10^{-8}$ M (vertical red line in Figure 2) for the native complex structure of Her2-Trastuzumab-Pertuzumab (PDB entry 6OGE), while the $K_d$ values between Her2 and pertuzumab Fab possess a much wider distribution, ranging from $1.9 \times 10^{-7}$ M to $2.9 \times 10^{-10}$ M, according to the Prodigy[22][23] calculations of the $3 \times 29{,}840$ homology structural models of the Her2-Trastuzumab-Pertuzumab complex (PDB entry 6OGE) with one site-specific missense mutation. Similarly, according to Table 3, the $K_d$ between Her2 and trastuzumab Fab is located at $4.9 \times 10^{-7}$ M (vertical red line in Figure 3) for the native complex structure of Her2-Trastuzumab-Pertuzumab (PDB entry 6OGE), while the $K_d$ values between Her2 and trastuzumab Fab also possess a much wider distribution, ranging from $2.5 \times 10^{-6}$ M to $1.7 \times 10^{-8}$ M, according to the Prodigy[22][23] calculations of the $3 \times 29{,}840$ homology structural models of the Her2-Trastuzumab-Pertuzumab complex (PDB entry 6OGE[14]) with one site-specific missense mutation.

| Binding partners | Scalable $K_d$ landscapes | Histograms of $K_d$ distributions |
|---|---|---|
| A + B | Table 3 (supplementary file) | Figure 1 (supplementary file) |
| A + C | Table 4 (supplementary file) | Figure 2 (supplementary file) |
| A + D | Table 5 (supplementary file) | Figure 3 (supplementary file) |
| A + E | Table 6 (supplementary file) | Figure 4 (supplementary file) |
| A + BC | Table 7 (supplementary file) | Figure 5 (supplementary file) |
| A + DE | Table 8 (supplementary file) | Figure 6 (supplementary file) |

**Table 4.** A summary of scalable Her2-Trastuzumab-Pertuzumab binding affinity landscapes and their distribution patterns. In this table, the supplementary file represents supps.pdf, and the codes (A, B, C, etc.) for binding partners are defined in Table 2.

Taken together, for both pertuzumab Fab and trastuzumab Fab, there is room for both increase and decrease in their antigen-antibody $K_d$ values, as shown in Figures 2 and 3. The two scalable antigen-antibody binding affinity landscapes (Figures 2 and 3) are like two guiding maps for antigen-antibody binding affinities, which is one inextricable factor in the equation of $y = f(x)$, where $x$ stands for the optimal $K_d$ or a range of it, while $y$ stands for the optimal efficacy and specificity of antibodies and ADCs[12][13]. Of interesting note, the HER2-Trastuzumab-Pertuzumab binding affinity landscapes (Figures 2 and 3) elucidate the binding affinity variations caused by site-specific mutations, such as the S911F mutation in chain C of the pertuzumab heavy chain, as demonstrated in the supplementary file fin.pdb and Figure 7 of the supplementary file supps.pdf. After the computational analysis on Wuxi Taihu Lake High Performance Computing platforms, this particular mutation S911F was also assessed using the Prodigy server[22][23], which returned an identical $K_d$ between chain A (Her2) and chain BC (Pertuzumab FAB, Table 2) of $2.9 \times 10^{-10}$ M (mutation No. 18214 in Table 7 of the supplementary file supps.pdf). This $K_d$ of $2.9 \times 10^{-10}$ M indicates an $\sim$ two orders of magnitude enhanced antigen-antibody binding affinity due to this particular mutation S911F, compared to the $K_d$ of $1.9 \times 10^{-8}$ M between Her2 and pertuzumab Fab in the native experimental Her2-Trastuzumab-Pertuzumab complex structure (PDB entry 6OGE[14]).

## Conclusion and Discussion

This study employs a scalable in silico workflow[29], integrating structural modeling[21] and physics-based $K_d$ calculations[22][23], to construct two scalable antigen-antibody binding affinity landscapes (Figures 2 and 3) using Her2-Trastuzumab-Pertuzumab (PDB entry 6OGE[14]) as a model system. This approach introduces one site-specific missense mutation, ensuring reasonable accuracy in defining these binding affinity landscapes (Figures 2 and 3)[21][22][23]. Of further interest, these scalable antigen-antibody binding affinity landscapes (Figures 2, 3, and supplementary information in Table 4) can be used the other way around, i.e., as a structural biophysics-based target-specific search engine[8] which takes as input a desired $K_d$ value or a range of it, and returns a list of $K_d$-ranked Trastuzumab or Pertuzumab analogues with potentially improved efficacy and/or specificity for Her2, offering a hopeful tool for the discovery and design of next-generation Her2-targeting ADCs[12][13]. In addition, the scalable workflow[29] described here presents a technically feasible method for generating synthetic structural and biophysical data, which is useful for enhancing the specificity and efficacy of therapeutic antibodies and ADCs[8][36]. Finally, incorporating databases such as PDB[27] and AFDB[37][38][39][40], this scalable in silico approach also supports the continued accumulation of synthetic structural and biophysical data for the development of AI models in drug discovery and design[5][6][41].

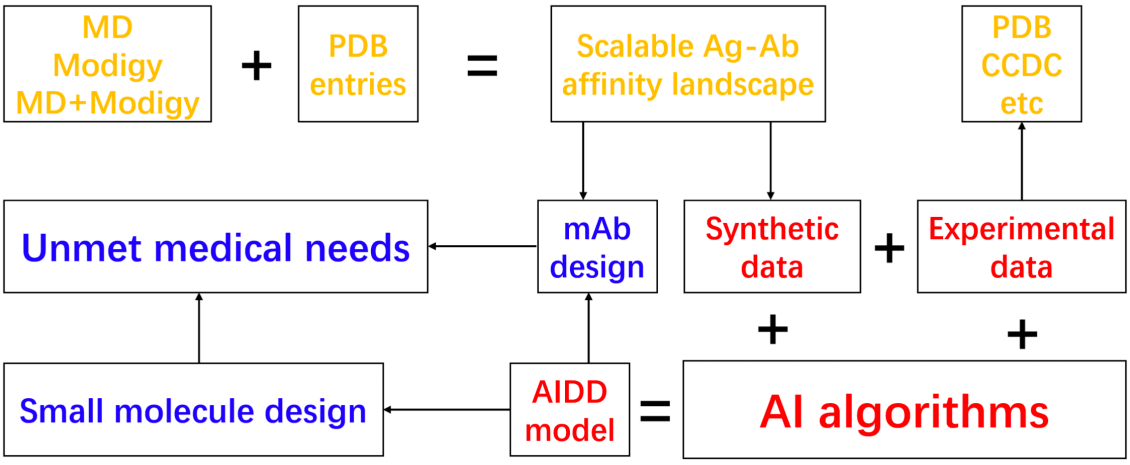


**Figure 4.** A flowchart depicting the generation of a scalable antigen-antibody binding affinity landscape for designing antibodies and small molecule compounds with improved efficacy and specificity. In this figure, Modigy represents the method approach combining Modeller and Prodigy for in silico generation of structural and intermolecular binding affinity data, as described in the Methods section.

Specifically, this study starts from an experimental Her2-Trastuzumab-Pertuzumab complex structure (PDB entry 6OGE[14]) to build two scalable antigen-antibody binding affinity landscapes (Figures 2 and 3), which are scalable because:

1. this Modigy (Figure 4) workflow[29] is broadly applicable to biomolecular structure databases such as PDB[27] and AFDB[37][38][39][40].
2. this Modigy (Figure 4) workflow[29] introduced only one site-specific missense mutation to the Her2-Trastuzumab-Pertuzumab complex structure (PDB entry 6OGE[14]), where the number could be larger, provided that the overall accuracy is reasonable for the synthetic structural and biophysical data[29].
3. the Her2-Trastuzumab-Pertuzumab binding affinity landscape (Figures 2 and 3) includes not only site-specific mutants of the two antibodies but also site-specific mutants of the target, i.e., Her2 as the antigen, highlighting the use of this in silico workflow[29] in the high-throughput generation of synthetic structural and biophysical data for other drug targets (GPCRs[42], ion channels[43], etc.) to train AI models for the discovery and design[8] of not just therapeutic antibodies and ADC, but also of small molecule compounds[44][45].
4. method-wise, in addition to the structural modeling[21] and physics-based $K_d$ calculations[22][23] employed here, this Modigy (Figure 4) workflow[29] is also able to integrate molecular dynamics simulations[46][47] to further enhance the accuracy of the structural biophysics-based $K_d$ calculations in drug discovery and design[48][49].

To sum up, this scalable synthetic structural and biophysics data serve two purposes: (1) this scalable Modigy (Figure 4) workflow[29] creates a scalable antigen-antibody binding affinity landscape, which acts like a map to guide the design of monoclonal antibodies or ADCs with optimal binding affinities[12][13]; (2) this scalable Modigy (Figure 4) workflow[29] generates useful training data[50][51] for AI-driven drug design (AIDD, Figure 4) models[5][6][8] towards the design of both monoclonal antibodies, ADCs[12][13] and small molecule compounds (Figure 4) with improved efficacy and specificity.

## Acknowledgments

The author is grateful to the communities of structural biology, biophysics, medicinal and computational chemistry, and algorithm design for the continued accumulation of knowledge and data for drug

discovery & design, and for the continued development of tools (hardware, software, and algorithms) for drug discovery & design.

## Supplementary Material

1. Supplementary file fin.pdb: a homology structural model of the Her2-Trastuzumab-Pertuzumab complex (PDB entry 6OGE) with one particular mutation S911F.
2. Supplementary file supps.pdf: supplementary tables and figures of the antigen-antibody binding affinity landscapes with ENHERTU's Trastuzumab as an example.

## References


1. ^*Charles Dumontet, Janice M. Reichert, Peter D. Senter, John M. Lambert, Alain Beck. (2023). Antibody–drug conjugates come of age in oncology. Nature Reviews Drug Discovery. 22(8):641–661.*
2. ^*Cindy H. Chau, Patricia S. Steeg, William D. Figg. (2019). Antibody–drug conjugates for cancer. The Lancet. 394(10200):793–804.*
3. ^*Puregmaa Khongorzul, Cai Jia Ling, Farhan Ullah Khan, Awais Ullah Ihsan, Juan Zhang. (2020). Antibody–drug conjugates: A comprehensive review. Molecular Cancer Research. 18(1):3–19.*
4. ^*Zhiwen Fu, Shijun Li, Sifei Han, Chen Shi, Yu Zhang. (2022). Antibody drug conjugate: The biological missile for targeted cancer therapy. Signal Transduction and Targeted Therapy. 7(1).*
5. a, b, c, d*Han van de Waterbeemd, Dennis A. Smith, Kevin Beaumont, Don K. Walker. (2001). Property-based design-optimization of drug absorption and pharmacokinetics. Journal of Medicinal Chemistry. 44(9):1313–1333.*
6. a, b, c, d*Lewis D. Pennington, Matthew J. Hesse, Dennis C. Koester, Rory C. McAtee, Alshaima'a M. Qunies, et al. (2024). Property-based drug design merits a nobel prize. Journal of Medicinal Chemistry.*
7. ^*Urmila Kulkarni-Kale, Snehal Raskar-Renuse, Girija Natekar-Kalantre, Smita A. Saxena. Antigen–antibody interaction database (AgAbDb): A compendium of antigen–antibody interactions. In: Immunoinformatics.: Springer New York 2014. pp. 149–164. ISBN 9781493911158*
8. a, b, c, d, e, f*Wei Li, Gary Vottevor. (2023). Towards a truly general intermolecular binding affinity calculator for drug discovery & design.*
9. ^*Reginald Evans, Greg M. Thurber. (2022). Design of high avidity and low affinity antibodies for in situ control of antibody drug conjugate targeting. Scientific Reports. 12(1).*

10. ^Guus A. M. S. van Dongen. (2021). Improving tumor penetration of antibodies and antibody–drug conjugates: Taking away the barriers for trojan horses. Cancer Research. 81(15):3956–3957.

11. ^Rita Khoury, Khalil Saleh, Nadine Khalife, Mohamad Saleh, Claude Chahine, et al. (2023). Mechanisms of resistance to antibody-drug conjugates. International Journal of Molecular Sciences. 24(11):9674.

12. a, b, c, d, eYiming Jin, Megan A. Schladetsch, Xueting Huang, Marcy J. Balunas, Andrew J. Wiemer. (2022). Stepping forward in antibody-drug conjugate development. Pharmacology & Therapeutics. 229:107917.

13. a, b, c, d, e, fJeffrey C. Kang, Wei Sun, Priyanka Khare, Mostafa Karimi, Xiaoli Wang, et al. (2019). Engineering a HER2-specific antibody–drug conjugate to increase lysosomal delivery and therapeutic efficacy. Nature Biotechnology. 37(5):523–526.

14. a, b, c, d, e, f, g, h, i, j, k, l, m, n, o, p, q, rYue Hao, Xinchao Yu, Yonghong Bai, Helen J. McBride, Xin Huang. (2019). Cryo-EM structure of HER2-trastuzumab-pertuzumab complex. Wenqing Xueditor. PLOS ONE. 14(5):e0216095.

15. a, b, c, d, e, fRémi Ruedas, Rémi Vuillemot, Thibault Tubiana, Jean-Marie Winter, Laura Pieri, et al. (2024). Structure and conformational variability of the HER2-trastuzumab-pertuzumab complex. Journal of Structural Biology. 216(2):108095.

16. ^Adrián Velázquez-Coy, Hiroyasu Ohtaka, Azin Nezami, Salman Muzammil, Ernesto Freire. (2004). Isothermal titration calorimetry. Current Protocols in Cell Biology. 23(1).

17. ^Wei Li. (2017). Gravity-driven pH adjustment for site-specific protein pKa measurement by solution-state NMR. Measurement Science and Technology. 28(12):127002.

18. ^Helen Webb, Barbara Mary Tynan-Connolly, Gregory M. Lee, Damien Farrell, Fergal OMeara, et al. (2010). Remeasuring HEWL pKa values by NMR spectroscopy: Methods, analysis, accuracy, and implications for theoretical pKa calculations. Proteins: Structure, Function, and Bioinformatics. 79(3):685–702.

19. ^Badreddine Douzi. Protein–protein interactions: Surface plasmon resonance. In: Bacterial protein secretion systems.: Springer New York 2017. pp. 257–275. ISBN 9781493970339

20. ^Christopher Lipinski, Andrew Hopkins. (2004). Navigating chemical space for biology and medicine. Nature. 432(7019):855–861.

21. a, b, c, d, e, f, g, h, i, j, kBenjamin Webb, Andrej Sali. Protein structure modeling with MODELLER. In: Methods in molecular biology.: Springer US 2020. pp. 239–255.

22. a, b, c, d, e, f, g, h, i, j, k, l, m, n, oAnna Vangone, Alexandre MJJ Bonvin. (2015). Contacts-based prediction of binding affinity in protein-protein complexes. eLife. 4.

23. a, b, c, d, e, f, g, h, i, j, k, l, m, n, oLi C. Xue, João Pglm Rodrigues, Panagiotis L. Kastritis, Alexandre Mjj Bonvin, A nna Vangone. (2016). PRODIGY: A web server for predicting the binding affinity of protein-protein complexe s. Bioinformatics. :btw514.

24. ^Susan J. Keam. (2020). Trastuzumab deruxtecan: First approval. Drugs. 80(5):501–508.

25. ^Jiyun Lee, Yeon Hee Park. (2021). Trastuzumab deruxtecan for HER2+ advanced breast cancer. Future Onc ology. 18(1):7–19.

26. ^Hiromi Okamoto, Masataka Oitate, Katsunobu Hagihara, Hideyuki Shiozawa, Yoshitake Furuta, et al. (202 0). Pharmacokinetics of trastuzumab deruxtecan (t-DXd), a novel anti-HER2 antibody-drug conjugate, in H ER2-positive tumour-bearing mice. Xenobiotica. 50(10):1242–1250.

27. a, b, cHelen Berman, Kim Henrick, Haruki Nakamura. (2003). Announcing the worldwide protein data bank. Nature Structural & Molecular Biology. 10(12):980–980.

28. ^Sriram Subramaniam, Gerard J. Kleywegt. (2022). A paradigm shift in structural biology. Nature Methods. 19(1):20–23.

29. a, b, c, d, e, f, g, h, i, j, kWei Li. (2024). In silico generation of structural and intermolecular binding affinity data with reasonable accuracy: Expanding horizons in drug discovery and design.

30. ^John F. Valliere-Douglass, Shawna M. Hengel, Lucy Y. Pan. (2014). Approaches to interchain cysteine-linked ADC characterization by mass spectrometry. Molecular Pharmaceutics. 12(6):1774–1783.

31. ^Ruud G. E. Coumans, Gerry J. A. Ariaans, Henri J. Spijker, Pascal Renart Verkerk, Patrick H. Beusker, et al. (2 020). A platform for the generation of site-specific antibody–drug conjugates that allows for selective reduc tion of engineered cysteines. Bioconjugate Chemistry. 31(9):2136–2146.

32. ^Grace H. Pham, Weijia Ou, Badry Bursulaya, Michael DiDonato, Ananda Herath, et al. (2018). Tuning a pro tein-labeling reaction to achieve highly site selective lysine conjugation. ChemBioChem. 19(8):799–804.

33. ^Nathaniel D. M. Holman, Anthony J. Wilkinson, Margaret C. M. Smith. (2021). Alanine-scanning mutagene sis of protein mannosyl-transferase from streptomyces coelicolor reveals strong activity-stability correlatio n. Microbiology. 167(10).

34. ^Xiyun Ye, Yen-Chun Lee, Zachary P. Gates, Yingjie Ling, Jennifer C. Mortensen, et al. (2022). Binary combin atorial scanning reveals potent poly-alanine-substituted inhibitors of protein-protein interactions. Commu nications Chemistry. 5(1).

35. ^Guanjie Li, Hiroyuki Suzuki, Tomohiro Tanaka, Teizo Asano, Takeo Yoshikawa, et al. (2023). Epitope mapp ing of an anti-EpCAM monoclonal antibody (EpMab-37) using the alanine scanning method. Monoclonal Antibodies in Immunodiagnosis and Immunotherapy. 42(1):41–47.

36. ^Dong Xu, Yang Zhang. (2011). Improving the physical realism and structural accuracy of protein models by a two-step atomic-level energy minimization. Biophys J. 101:2525–2534.

37. a, bJohn Jumper, Richard Evans, Alexander Pritzel, Tim Green, Michael Figurnov, et al. (2021). Highly accurat e protein structure prediction with AlphaFold. Nature. 596(7873):583–589.

38. a, bAlexander B. Tong, Jason D. Burch, Daniel McKay, Carlos Bustamante, Michael A. Crackower, et al. (2021). Could AlphaFold revolutionize chemical therapeutics? Nature Structural & Molecular Biology. 28(10):771–77 2.

39. a, bKiersten M. Ruff, Rohit V. Pappu. (2021). AlphaFold and implications for intrinsically disordered proteins. Journal of Molecular Biology. :167208.

40. a, bMatthew K. Higgins. (2021). Can we AlphaFold our way out of the next pandemic? Journal of Molecular Biology. :167093.

41. ^Christine E. Tinberg, Sagar D. Khare, Jiayi Dou, Lindsey Doyle, Jorgen W. Nelson, et al. (2013). Computation al design of ligand-binding proteins with high affinity and selectivity. Nature. 501(7466):212–216.

42. ^Mingyang Zhang, Ting Chen, Xun Lu, Xiaobing Lan, Ziqiang Chen, et al. (2024). G protein-coupled recepto rs (GPCRs): Advances in structures, mechanisms, and drug discovery. Signal Transduction and Targeted The rapy. 9(1).

43. ^R. W. Tsien, P. Hess, E. W. McCleskey, R. L. Rosenberg. (1987). Calcium channels: Mechanisms of selectivity, p ermeation, and block. Annual Review of Biophysics and Biophysical Chemistry. 16(1):265–290.

44. ^Wei Li, Ganggang Shi. (2019). How CaV1.2-bound verapamil blocks Ca2+ influx into cardiomyocyte: Atomi c level views. Pharmacological Research. 139:153–157.

45. ^Wei Li. (2020). Calcium channel trafficking blocker gabapentin bound to the - subunit of voltage-gated ca lcium channel: A computational structural investigation.

46. ^Wei Li. (2016). Characterising the interaction between caenopore-5 and model membranes by NMR spectr oscopy and molecular dynamics simulations. {PhD} thesis, University of Auckland.

47. ^Xing Du, Yuping Li, Yong Xia, Jingwei Ai, Yinghao Wu. (2017). Molecular dynamics simulations and free en ergy calculations of protein–ligand interactions: Recent advances and future perspectives. Current pharma ceutical design. 23(30):4436–4450.

48. ^Rohan Gupta, Devesh Srivastava, Mehar Sahu, Swati Tiwari, Rashmi K. Ambasta, et al. (2021). Artificial in telligence to deep learning: Machine intelligence approach for drug discovery. Molecular Diversity. 25(3):131 5–1360.

49. ^ *Jean-Yves Trosset, Christian Cavé. In silico drug-target profiling. In: Target identification and validation in drug discovery.: Springer New York 2019. pp. 89–103.*

50. ^ *T. Liu, Y. Lin, X. Wen, R. N. Jorissen, M. K. Gilson. (2007). BindingDB: A web-accessible database of experim entally determined protein-ligand binding affinities. Nucleic Acids Research. 35(Database):D198–D201.*

51. ^ *Renxiao Wang, Xueliang Fang, Yipin Lu, Chao-Yie Yang, Shaomeng Wang. (2005). The PDBbind database: Methodologies and updates. Journal of Medicinal Chemistry. 48(12):4111–4119.*

**Supplementary data:** available at https://doi.org/10.32388/I2P70W

## Declarations

**Funding:** No specific funding was received for this work.

**Potential competing interests:** No potential competing interests to declare.